On the Use of Evanescent Electromagnetic Waves in the Detection and Identification of Objects Buried in Lossy Soil

Glenn S. Smith, *Fellow, IEEE,* and L. E. Rickard Petersson, *Student Member, IEEE*

***Abstract*—In some electromagnetic (EM) systems proposed for the detection of buried objects, such as landmines, the transducers (antennas) are located very close to the surface of the earth. The coupling of energy into the earth is then by the near field of the transducers, or, more precisely, by evanescent waves as well as propagating waves in the spectrum for the radiation from the transducers. Evanescent waves also contribute to the coupling of the scattered field from the shallowly buried object to the transducers. In this paper, we use simple models based on a plane-wave spectral analysis to perform a preliminary examination of the role that evanescent waves can play in the detection and identification of the buried object. The degree to which features in the image of the object can be resolved is of particular interest, since the features can be used to distinguish the object from clutter (such as rocks). The effect of loss in the soil on imaging is also of interest.**

***Index Terms*—Evanescent waves, ground-penetrating radar, imaging, landmine detection.**

I. Introduction

FIG. 1 is a schematic drawing for a generic electromagnetic (EM) system for locating objects such as landmines buried in the earth. The basic principle of operation is fairly simple: A transducer produces an incident EM signal (incident field); this signal causes an EM response in the buried object (electric current, electric polarization, or magnetic polarization) that, in turn, produces the scattered EM signal (scattered field). The scattered signal is measured by a second transducer and processed to detect and identify the object. Two separate transducers, a transmitter and a receiver as in Fig. 1, may be used, or a single transducer may provide both functions. The frequency of operation for such systems ranges from below 1 MHz (metal detectors with coils as the transducers) to above 1 GHz (ground-penetrating radars with antennas as the transducers) [1]–[4].

A successful system must be able to detect and identify the buried object. Detection simply means locating a buried object; the object could be a landmine, a rock, or simply a change in soil type. Identification implies the ability to distinguish between these possibilities. An important consideration then is the quality of the unprocessed information collected by the system that can be used for both detection and identification. The receiving transducer in Fig. 1 measures the scattered field at the height h above the surface of the earth. Backpropagation may be used to transfer this field to the surface of the earth or even into the earth to the depth d of the object. However, objects are often buried in soil with unknown properties, so backpropagation below the surface may be impractical. Then the best that can be accomplished is to provide an accurate measure of the scattered field at the surface of the earth. This is shown schematically in Fig. 2.

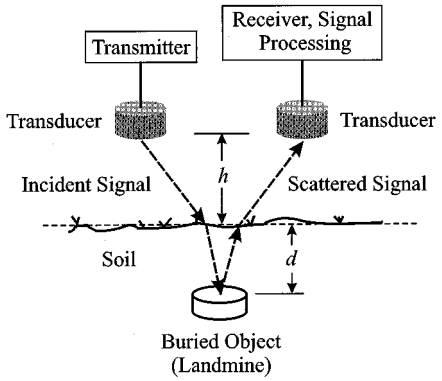

Fig. 1. Schematic drawing for a generic EM system for locating objects buried in the earth.

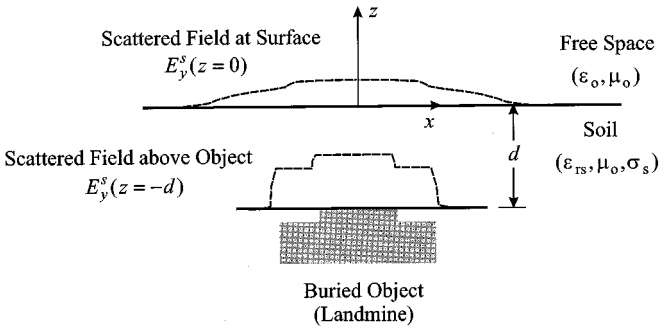

Fig. 2. Sketch showing the scattered field on a plane above the object and at the surface of the earth.

The smallest feature that can be distinguished in the scattered field is important, because it determines the resolution of any "image" that may be constructed to identify the buried object.[1] The smallest feature that can be distinguished is determined by

Manuscript received August 16, 1999; revised March 6, 2000. This work was supported by the Army Research Office under Contracts DAAG55-98-1-0403 and DAAH04-96-1-0448.

The authors are with the School of Electrical and Computer Engineering, Georgia Institute of Technology, Atlanta, GA 30332-0250 USA (glenn.smith@ece.gatech.edu).

Publisher Item Identifier S 0018-926X(00)09343-1.

[1]Here we are only concerned with identification by imaging. Identification, however, can be accomplished by other means; for example, a distinctive frequency response can be used to discriminate between a specific buried object and clutter [5].

many factors, not the least of which is the frequency or wavelength ($\lambda_o = c/f$) at which the system operates. However, for detection of the object, the wavelength does not have to be small compared to the dimensions of the object. A metal detector operating at a wavelength that is one thousand times the maximum dimension of a metallic object can detect the object, as can a radar operating at a wavelength that is one tenth the maximum dimension of the object [6]–[9].

The transducers (antennas) in a system for detecting buried objects, such as the one shown in Fig. 1, are sometimes located very close to the surface of the earth, $h < \lambda_o/4$ [10]–[13]. The coupling of energy into the earth is then by the near field of the transducers, or, more precisely, by evanescent waves (inhomogeneous waves) as well as propagating waves (homogeneous waves) in the spectrum for the radiation from the transducers. Evanescent waves also contribute to the coupling of the scattered field from the shallowly buried object to the transducers. In this case, the interpretation of the arrows in Fig. 1 as optical rays may then be inappropriate, and a more complex model for the propagation may be required.

In this paper, we will use simple analytical models to perform a preliminary examination of the role evanescent waves can play in the detection and identification of shallowly buried objects such as landmines.

II. Spectral Representation-Evanescent and Propagating Waves

In the analysis that follows, we will only consider two-dimensional configurations; with reference to Fig. 2, all geometrical and electrical quantities will be assumed invariant with respect to y. We will also assume that the field is TE, which, in this notation, means that the field has only the components E_y, H_x, H_z. Harmonic time dependence is used, and the factor $e^{j\omega t}$ is suppressed throughout. The electrical properties of the nonmagnetic ($\mu_s = \mu_o$) soil containing the buried object are the relative permittivity ε_{rs} and the conductivity σ_s or loss tangent $p_s = \sigma_s/\omega\varepsilon_{rs}\varepsilon_o$.

A component of the scattered EM field on a plane surface just above the buried object at $z = -d$ can be expressed as the Fourier transform of a spectral function [14], [15]. For example, for the component E_y^s we have

$$E_y^s(x, z=-d) = \frac{1}{2\pi}\int_{-\infty}^{\infty} F_y(k_x)e^{-jk_x x}\,dk_x \tag{1}$$

with the spectral function

$$F_y(k_x) = \int_{-\infty}^{\infty} E_y^s(x, z=-d)e^{jk_x x}\,dx. \tag{2}$$

When the right-hand side of (1) is interpreted as a summation of plane waves (a plane wave spectrum) evaluated at the plane $z = -d$, the scattered field in the soil above the object becomes

$$E_y^s(x, z) = \frac{1}{2\pi}\int_{-\infty}^{\infty} F_y(k_x)e^{-jk_z^s d}e^{-j\vec{k}^s\cdot\vec{r}}dk_x, \quad -d \le z \le 0 \tag{3}$$

where the complex vector wave number in the soil is

$$\vec{k}^s = k_x\hat{x} + k_z^s\hat{z} \tag{4}$$

with

$$k_z^s = \beta_z^s - j\alpha_z^s = \sqrt{k_s^2 - k_x^2} = k_o\sqrt{[\varepsilon_{rs} - (k_x/k_o)^2] - j\varepsilon_{rs}p_s} \tag{5}$$

and $k_o = \omega/c$. Now the scattered field above the surface of the earth in free space is simply[2]

$$E_y^s(x, z) = \frac{1}{2\pi}\int_{-\infty}^{\infty} T_\perp(k_x)F_y(k_x)e^{-jk_z^s d}e^{-j\vec{k}^t\cdot\vec{r}}\,dk_x, \quad z \ge 0 \tag{6}$$

where the plane-wave transmission coefficient for TE polarization is [15], [16]

$$T_\perp(k_x) = \frac{2k_z^s}{k_z^s + k_z^t} \tag{7}$$

and the vector wave number in free space is

$$\vec{k}^t = k_x\hat{x} + k_z^t\hat{z} \tag{8}$$

with

$$\begin{aligned} k_z^t &= \beta_z^t = \sqrt{k_o^2 - k_x^2}, \quad 0 \le k_x^2 \le k_o^2, \quad \text{Propagating Wave} \\ &= -j\alpha_z^t = -j\sqrt{k_x^2 - k_o^2}, \quad k_x^2 > k_o^2, \quad \text{Evanescent Wave.} \end{aligned} \tag{9}$$

In free space, waves with $k_x^2 \le k_o^2$ propagate in the z direction as $\exp(-j\beta_z^t z)$, while waves with $k_x^2 > k_o^2$ evanesce or decay in the z direction as $\exp(-\alpha_z^t z)$. When there is loss in the soil ($\sigma_s \neq 0$), all waves in the soil decay in the z direction, so it is not possible to clearly divide the range for k_x into portions corresponding to propagating and evanescent waves. However, a rough estimate for this division can be obtained from the lossless case ($\sigma_s = 0$), where $k_x^2 \le \varepsilon_{rs}k_o^2$ for propagating waves and $k_x^2 > \varepsilon_{rs}k_o^2$ for evanescent waves.

We will ignore any multiple scattering of the field between the object and the surface of the earth, so (6) is the only field in free space due to the presence of the buried object. This is the field that the system must measure and process to detect and identify the buried object.

The geometrical and electrical properties of the buried object determine the spatial features (variation in x) of the scattered field on the plane just above the object (1). These features are characterized by the range of the transverse wave number $k_x = 2\pi/\lambda_x$ over which the spectral function F_y is significant: $|k_x| \le k_{x\max}$ ($\lambda_x \ge \lambda_{x\min}$). The smaller the features the larger $k_{x\max}$ (the smaller $\lambda_{x\min}$). Clearly, we want these same features to appear in the field measured at or above the surface of the earth. This means that the additional factor that appears in (6) but not in (1); that is

$$T_\perp(k_x)e^{-j\beta_z^s(k_x)d}e^{-\alpha_z^s(k_x)d}e^{-j\beta_z^t(k_x)z}e^{-\alpha_z^t(k_x)z} \tag{10}$$

must not become too small over the range $|k_x| \le k_{x\max}$.

The dominant term in (10) is often the exponential attenuation $\exp[-\alpha_z^s(k_x)d]\exp[-\alpha_z^t(k_x)z]$. As mentioned above, this attenuation can be due to the wave being evanescent (for a particular value of k_x) either in free space or in the soil, or it can be

[2]This is the scattered field of the buried object. It does not include the incident field of the transmitter or the reflection of this field from the surface of the earth.

due to the dissipation in the soil ($\sigma_s \neq 0$). The attenuation for evanescent waves in free space can be reduced by measuring the field close to the surface of the earth ($z \approx 0$), so the attenuation in the soil, namely the factor $\alpha_z^s(k_x)$ in the exponent, is most important. To simplify the discussion of this factor, we introduce a frequency-independent normalized loss tangent for the soil

$$P_s = \frac{k_o}{k_x} p_s = \frac{\zeta_o \sigma_s}{\varepsilon_{rs} k_x} \tag{11}$$

where $\zeta_o = \sqrt{\mu_o/\varepsilon_o}$ is the wave impedance of free space. Notice that when k_x is fixed, P_s is the loss tangent p_s at the frequency for which $k_o = \omega/c = k_x$. Now (5) can be written as

$$\begin{aligned} k_z^s/k_x &= \beta_z^s/k_x - j\alpha_z^s/k_x \\ &= \sqrt{\left[\left(\frac{k_o}{k_x}\right)^2 \varepsilon_{rs} - 1\right] - j\varepsilon_{rs} P_s \left(\frac{k_o}{k_x}\right)}. \end{aligned} \tag{12}$$

The normalized attenuation constant α_z^s/k_x is graphed as a function of the normalized wave number, k_o/k_x, in Fig. 3. Results are shown for soil with relative permittivity $\varepsilon_{rs} = 9$ and five different values of the loss parameter: $P_s = 0.0, 0.1, 0.4, 0.8$, and 1.6. A convenient way to interpret this graph is to assume that k_x is fixed and that the wave number in free space $k_o = \omega/c$ (the frequency) is varied. For example, k_x could be fixed at the value $k_{x\max}$ associated with the smallest feature of a buried object. The bars below the figure show the ranges of wave number for which a wave is propagating or evanescent in free space and in the lossless soil. Notice that there is no attenuation in free space until k_o/k_x is below 1.0, and there is no attenuation in the lossless soil ($P_s = 0$) until k_o/k_x is below the value $1/\sqrt{\varepsilon_{rs}} = 0.33$. Also, notice that some waves that evanesce in free space propagate in the soil.

First, we will consider the case where the soil is lossless, the curve for $P_s = 0.0$ in Fig. 3. For point A ($k_o/k_x = 1.5$), the wave is propagating in both free space and in the soil; for point B ($k_o/k_x = 0.75$), the wave is evanescent in free space and propagating in the soil; and for point C ($k_o/k_x = 0.25$), the wave is evanescent in both free space and in the soil. For soil with low loss, for example the curve for $P_s = 0.1$ in Fig. 3, the situation is similar to that for lossless soil. Only now there is a small, almost constant, value of attenuation in the soil when $k_o/k_x > 1/\sqrt{\varepsilon_{rs}} = 0.33$, and the transition to evanescence is smoother than for lossless soil.

Now we will consider the other extreme, the case where the soil is very lossy, the curve for $P_s = 1.6$ in Fig. 3. The features that distinguished the regions for propagation and evanescence in soil with low loss are now absent. The attenuation is seen to be a monotonically increasing function of k_o/k_x. Notice that the attenuation for point C is less than that for point A. Thus, a frequency at which the wave is evanescent (decays) in both regions (e.g., point C) appears to be the best choice. Recall that we have assumed that the attenuation in the soil is the dominant factor, because the attenuation in free space can be reduced by placing the transducers close to the surface of the earth.

This last result may seem surprising, we are purposefully using a wave that naturally evanesces (attenuates even when there is no loss in the soil) in both regions to reduce the overall attenuation of the wave. The cause of this phenomenon is fairly simple: When we decrease the frequency, we increase attenuation because the wave becomes evanescent; however, we also decrease attenuation because the soil becomes less dissipative; the latter is a bigger effect than the former.

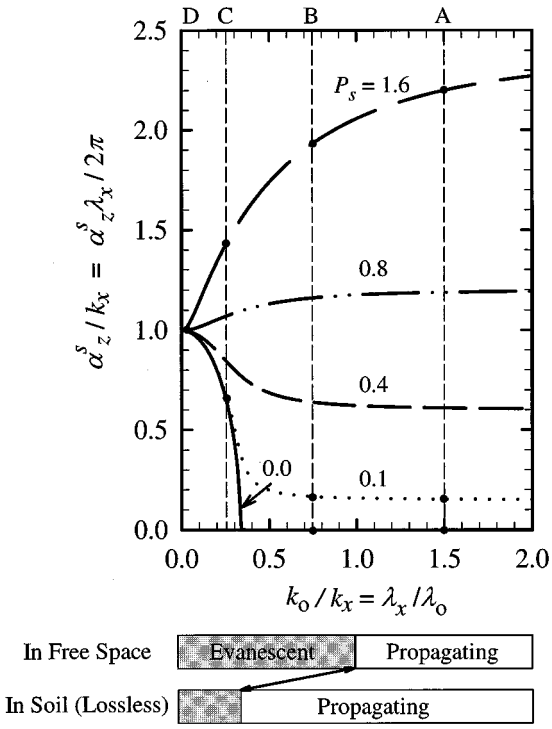

Fig. 3. Normalized attenuation constant in the soil as a function of the normalized wave number $\varepsilon_{rs} = 9$.

For the special value $P_s = 2/\sqrt{\varepsilon_{rs}}$, the normalized attenuation α_z^s/k_x given in (12) is independent of k_o/k_x. If the curve for this value ($P_s = 0.67$) were plotted in Fig. 3, it would be a horizontal straight line. Thus, to obtain a reduction in attenuation by reducing k_o/k_x, the curve for P_s must be above this line or

$$\sqrt{\varepsilon_{rs}} P_s/2 > 1. \tag{13}$$

Notice for this case, a reduction in k_o/k_x can never make α_z^s/k_x less than 1.0. So we are always dealing with extreme attenuation when (13) applies, for $\exp(-\alpha_z^s/k_x) \geq \exp(-1) = 0.368 = -8.7$ dB.

III. Simple Example Comparing the Resolution Obtained with Propagating and Evanescent Waves

The numerical results presented in the last section are for a single plane wave. To see how the ideas developed there apply to a spectrum of plane waves, the simple model for a detection system, shown in Fig. 4, is analyzed. Here, the source (transmitter) is a filament of current I_o at height h above the surface of the earth. The observation point (receiver) is located below the source at height g above the surface of the earth. This combination of transmitter and receiver will be referred to as the detector. The buried object, at depth d, is a pair of parallel, electrically thin, perfectly conducting wires of radius a, separated by

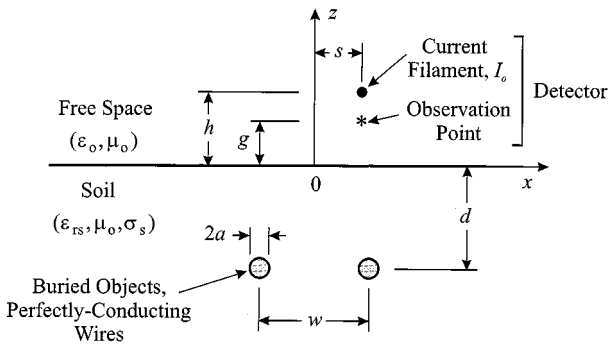

Fig. 4. Geometry for a simple model of a detection system.

the distance w. Notice that the buried wires are symmetrically located about $x = 0$, while the detector is displaced at $x = s$.

In this model, the current filament produces the TE incident field (E_y^i, H_x^i, H_z^i). The plane-wave spectrum for this field is obtained and allowed to propagate into the earth. The electric field $E_{y,\,\mathrm{soil}}^i(x = \pm w/2,\, z = -d)$ at the location of the wires is obtained, and the current in the perfectly conducting thin wires is estimated to be [17]

$$I_s = \frac{2\pi E_{y,\,\mathrm{soil}}^i(x = \pm w/2,\, z = -d)}{j\omega\mu_o \ln(k_s a)}. \tag{14}$$

The plane-wave spectrum for the scattered field produced by these currents is obtained and allowed to propagate into free space. The field component $H_x^s(s,\, g)$ at the detector is then used to evaluate the ability of the system to resolve the locations of the buried wires.

The important dimension in this analysis is the spacing w between the two buried wires. Therefore, we define our critical transverse wave number (transverse wavelength) associated with imaging the wires to be $k_{xw} = 2\pi/\lambda_{xw} = 2\pi/w$. The parameter $k_o/k_x = k_o/k_{xw} = w/\lambda_o$ that we use with Fig. 3 is then equal to the separation of the wires in terms of the free space wavelength.

As before, we will look at two extreme cases from Fig. 3, soil with low loss $P_s = 0.1$ and soil with very high loss $P_s = 1.6$. We consider the points marked $A - D$ for these two cases. For convenience, the values of k_o/k_{xw} and the spacings between the wires, w, in terms of the free space wavelength, λ_o, and in terms of the wavelength in the soil, λ_s, are given for these points in Table I.

In Fig. 5(a), the magnitude of the normalized scattered field $|H_x^s(s,\, g)w/I_o|$ is graphed as a function of the lateral position of the detector s/w. Each curve in the figure represents a scan of the detector over the surface of the earth. The parameters for this example are $h/w = 0.5$, $a/w = 0.05$, $d/w = 0.5$, $g/w = 0$ (detector at the surface of the earth) and the *soil with low loss* $\varepsilon_{rs} = 9$ and $P_s = 0.1$ (the second curve from the bottom in Fig. 3). For case A, the wires are separated by 1.5 wavelengths in free space and 4.5 wavelengths in the soil. The resolution of the locations of the two wires at $s/w = -0.5$ and $s/w = +0.5$ (vertical dash dot lines) is masked by a strong ripple that is caused by the interference of the scattered fields from the two wires.

TABLE I
PARAMETERS FOR EXAMPLE

Case	k_o / k_{xw}	w / λ_o	w / λ_s	
			$P_s = 0.1$	$P_s = 1.6$
A	1.50	1.50	4.50	4.99
B	0.75	0.75	2.26	2.91
C	0.25	0.25	0.76	1.45
D	0.025	0.025	0.12	0.43

The situation for case B is similar to that for case A, only the period of the ripple is longer, because the wires are now only separated by 0.75 wavelengths in free space and 2.3 wavelengths in the soil. For case C, the wires are separated by 0.25 wavelengths in free space and 0.76 wavelengths in the soil. The longer wavelength in the soil and the increased attenuation in the soil have just about eliminated the ripple, and the locations of the two wires are clearly resolved. Notice from Fig. 3 that the attenuation in the soil for case C is considerably greater than that for cases A and B. However, the received field for case C is only about a factor of four less than that for cases A and B (note the multiplication factor on the graph). For case D, the wires are only separated by 0.025 wavelengths in free space and 0.12 wavelengths in the soil. However, their locations are still resolved, albeit not as clearly as for case C.

The results in Fig. 5(b) are for the same geometrical parameters as for Fig. 5(a) but for the *soil with high loss* $\varepsilon_{rs} = 9, P_s = 1.6$ (the top curve in Fig. 3). The locations of the two wires are clearly resolved in all four cases: $A - D$. Notice from the multiplication factors on the graphs, that, as expected from Fig. 3, the amplitude of the received field is greatest for case D: about 100 times greater than for case C, 3 000 times greater than for case B, and 20 000 times greater than for case A.

The results in Fig. 5(b), particularly those for cases C and D, show that in lossy soil, the inclusion of evanescent waves in the spectrum can increase the amplitude of the received signals significantly without seriously affecting the ability to resolve the locations of the buried objects.

The results in Fig. 5 are for the detector at the surface of the earth, that is, $g = 0$. In Fig. 6, the normalized field for case C is shown as a function of the height of the detector, $0 \le g/w \le h/w = 0.5$. Fig. 6(a) is for the soil with low loss $P_s = 0.1$, and Fig. 6(b) is for the soil with very high loss $P_s = 1.6$. The resolution of the locations of the two wires is seen to decrease as the detector is raised above the surface of the earth. This is the result of the attenuation of the evanescent waves as well as the divergence of the propagating waves for the spectrum in free space.

IV. CONCLUSION

In some EM systems proposed for detecting shallowly buried objects, the transducers (antennas) are located very close to the surface of the earth. The coupling of energy into and out of the earth can then involve both the evanescent and the propagating waves in the plane wave spectrum for the radiation. The operating frequency can be chosen so that either the propagating waves or the evanescent waves dominate the spectrum in the range used for imaging the object. For the former, the operating

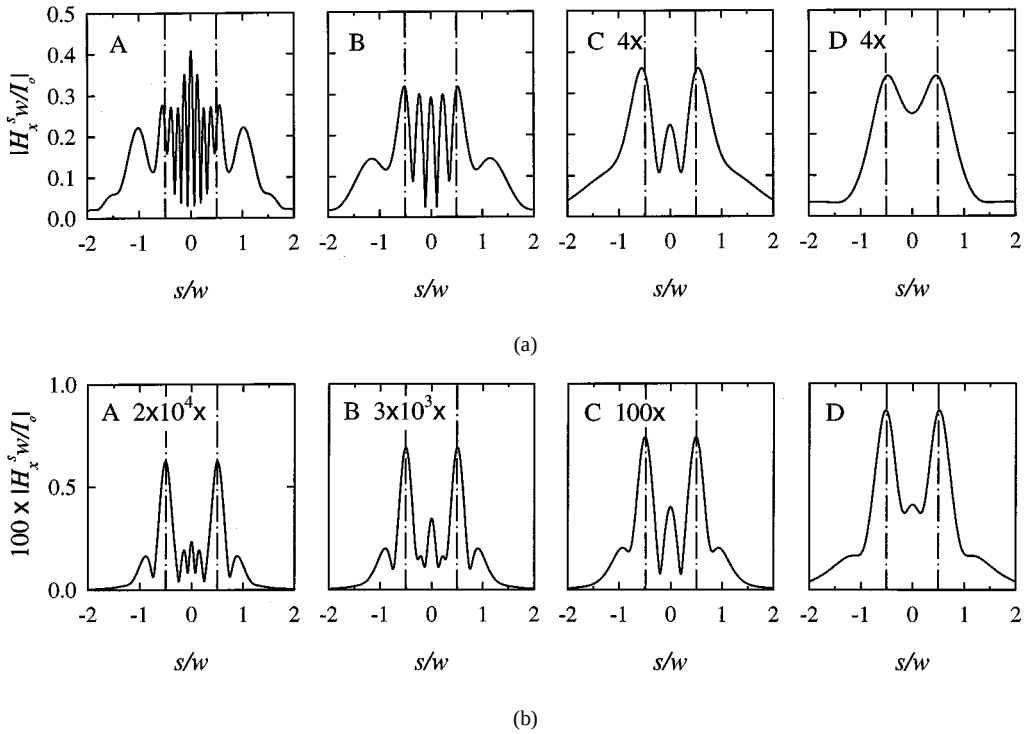

Fig. 5. The scattered magnetic field H_x^s of the two buried wires as the detector is scanned over the surface of the earth, for A. $k_o/k_{xw} = 1.5$, B. 0.75, C. 0.25, and D. 0.025. $h/w = 0.5$, $g/w = 0.0$, $d/w = 0.5$, $\varepsilon_{rs} = 9$. (a) Soil with low loss $P_s = 0.1$. (b) Soil with high loss $P_s = 1.6$.

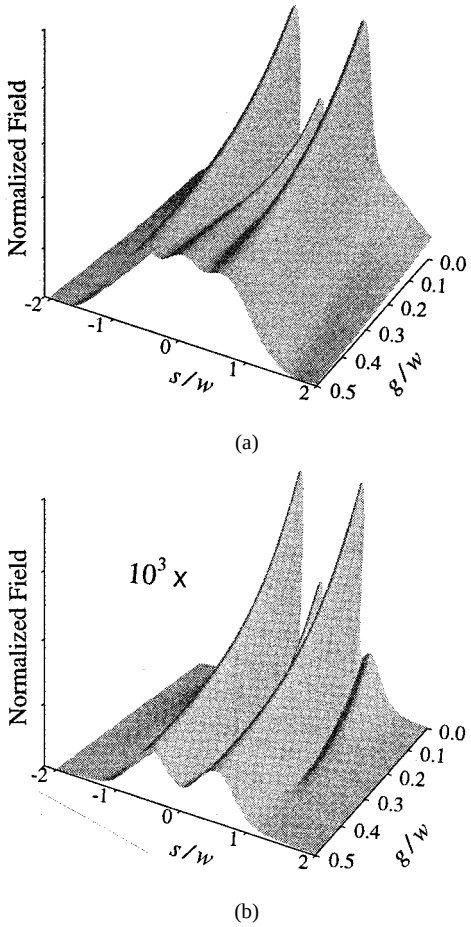

Fig. 6. The scattered magnetic field H_x^s for case C as a function of the height of the detector above the surface of the earth g/w. (a) Soil with low loss $P_s = 0.1$. (b) Soil with high loss $P_s = 1.6$.

frequency (a high frequency) is chosen so that the free-space wavelength is less than the dimensions of the object, while for the latter the operating frequency (a low frequency) is chosen so that the free-space wavelength is much greater than the dimensions of the object.

The results presented in this paper, which are based on simple analytical models, show that under the right conditions, the inclusion of evanescent waves in the spectrum can increase the amplitude of the received signals significantly without seriously affecting the ability to resolve the locations of the buried objects. The design of an actual detector (other than a metal detector) that specifically makes use of evanescent waves to detect buried objects is a project for future study.

An interesting observation from the analysis is that when k_{xw} (the resolution) is held fixed and the soil is very lossy, the attenuation of the evanescent waves at low frequencies, which is due to both natural decay and loss, can be less than the attenuation for the propagating waves at high frequencies, which is due to only the loss. For a soil with a frequency independent conductivity σ_s, this occurs whenever

$$\sqrt{\varepsilon_{rs}} P_s/2 = \frac{\zeta_o \sigma_s w}{4\pi\sqrt{\varepsilon_{rs}}} \approx \frac{30\sigma_s w}{\sqrt{\varepsilon_{rs}}} > 1 \tag{15}$$

where w is the dimension of the feature in the buried object that must be resolved. It should be emphasized, however, that this phenomenon only occurs in cases where there is extreme attenuation in the soil; that is, when $\exp(-\alpha_z^s w/2\pi) \geq \exp(-1) = 0.368 = -8.7$ dB.

For soil with a conductivity that increases with the frequency, which is the case for many soils at radio and microwave frequencies, the reduction in attenuation gained by use of the evanescent

spectrum (going to lower operating frequency) will be greater than indicated by the simple analysis presented in this paper [18]. This can be seen from Fig. 3. Consider a low frequency with low attenuation such as the point for $k_o/k_x = 0.75$ on the curve for $P_s = 0.1$. When the conductivity is independent of the frequency, the attenuation remains roughly constant as the frequency is increased, for example to the point $k_o/k_x = 1.5$. If the conductivity increases with the frequency, however, the value of P_s at $k_o/k_x = 1.5$ would increase, for example from 0.1 to 0.4, and the attenuation would increase.

The use of the evanescent spectrum to image a buried object is similar to what is done in near-field scanning optical microscopy (NSOM). In optical microscopy, the maximum frequency (minimum wavelength) of operation is fixed and evanescent waves are introduced to increase the resolution beyond that possible with a traditional microscope; that is, one that uses only propagating waves [19].

ACKNOWLEDGMENT

The senior author (G. Smith) first met Jim Wait when the author was a graduate student in the late 1960's. Earlier, Jim had published some results on the subject of the author's Ph.D. dissertation: the insulated loop antenna in a dissipative medium. The author is most grateful for the support and encouragement Jim provided to him over the past 30 years.

The authors would like to thank R. Apfeldorfer for his help during the early stage of this investigation.

REFERENCES

[1] "Basic studies—Detecting, destroying or inactivating mines," Final Rep. U.S. Army Eng. Ctr., Fort Belvoir, VA, Eng-1773, Nov. 1953.

[2] C. Stewart, "Summary of mine detection research," vol. 1, 2; U.S. Army Eng. Res. Development Lab., Fort Belvoir, VA, Tech. Rep. 1663, May 1960.

[3] R. V. Nolan, H. C. Egghart, L. Mittleman, R. L. Brooke, F. L. Roder, and D. L. Gravitte, "MERADCOM mine detection program 1960-1980," U.S. Army Mobility Equipment Res. Development Command, Fort Belvoir, VA, Rep. 2294, Mar. 1980.

[4] C. E. Baum, Ed., *Detection and Identification of Visually Obscured Targets*. London, U.K.: Taylor and Francis, 1998.

[5] N. Geng, P. Garber, L. Collins, and L. Carin, "Wideband electromagnetic induction for metal-target identification: Theory, measurement and signal processing," *Proc. SPIE: Detection and Remediation Technologies for Mines and Minelike Targets III*, vol. 3392, pp. 42–51, 1998.

[6] J. R. Wait, *Geo-Electromagnetism*. New York: Academic, 1982.

[7] D. J. Daniels, *Surface-Penetrating Radar*. London, U.K.: Inst. Elect. Eng., 1996.

[8] J. M. Bourgeois and G. S. Smith, "A fully three-dimensional simulation of a ground-penetrating radar: FDTD theory compared with experiment," *IEEE Trans. Geosci. Remote Sensing*, vol. 34, pp. 36–44, Jan. 1996.

[9] T. P. Montoya and G. S. Smith, "Land mine detection using a ground-penetrating radar based on resistively loaded vee dipoles," *IEEE Trans. Antennas Propagat.*, vol. 47, pp. 1795–1806, Dec. 1999.

[10] D. A. Hill, "Electromagnetic scattering by buried objects of low contrast," *IEEE Trans. Geosci. Remote Sensing*, vol. 26, pp. 195–203, Mar. 1988.

[11] ——, "Near-field detection of buried dielectric objects," *IEEE Trans. Geosci. Remote Sensing*, vol. 27, pp. 364–368, July 1989.

[12] L. S. Riggs and C. A. Amazeen, "Research with the waveguide below cutoff or separated aperture dielectric anomaly detection scheme," U.S. Army, Belvoir Res. Development Engrg. Ctr., Fort Belvoir, VA, Tech. Rep. 2497, Aug. 1990.

[13] J. M. Bourgeois and G. S. Smith, "A complete electromagnetic simulation of the separated-aperture sensor for detecting buried land mines," *IEEE Trans. Antennas Propagat.*, vol. 46, pp. 1419–1426, Oct. 1998.

[14] G. S. Smith, *An Introduction to Classical Electromagnetic Radiation*. Cambridge, U.K.: Cambridge Univ. Press, 1997.

[15] J. R. Wait, *Electromagnetic Waves in Stratified Media*. New York: Pergamon, 1962.

[16] G. S. Smith, "Directive properties of antennas for transmission into a material half-space," *IEEE Trans. Antennas Propagat.*, vol. AP-32, pp. 232–246, Mar. 1984.

[17] R. F. Harrington, *Time-Harmonic Electromagnetic Fields*. New York: McGraw-Hill, 1961.

[18] R. W. P. King and G. S. Smith, *Antennas in Matter: Fundamentals, Theory and Applications*. Cambridge, MA: MIT Press, 1981, ch. 6.

[19] M. A. Paesler and P. J. Moyer, *Near Field Optics*. New York: Wiley, 1996.

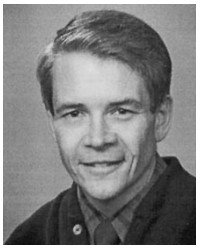

Glenn S. Smith (S'65–M'72–SM'80–F'86) received the B.S.E.E. degree from Tufts University, Medford, MA, in 1967, and the S.M. and Ph.D. degrees in applied physics from Harvard University, Cambridge, MA, in 1968 and 1972, respectively.

From 1972 to 1975, he served as a Postdoctoral Research Fellow at Harvard University and also as a part-time Research Associate and Instructor at Northeastern University, Boston, MA. In 1975, he joined the faculty of the School of Electrical and Computer Engineering at the Georgia Institute of Technology, Atlanta, GA, where he is currently Regents' Professor and John Pippin Chair in Electromagnetics. He is the author of *An Introduction to Classical Electromagnetic Radiation* (Cambridge, MA: Cambridge Univ. Press, 1997) and coauthor of *Antennas in Matter: Fundamentals, Theory and Applications*, (Cambridge, MA: MIT Press, 1981). He also authored the chapter "Loop antennas," in *Antenna Engineering Handbook* (New York: McGraw-Hill, 1993). His technical interests include basic electromagnetic theory and measurements, antennas and wave propagation in materials, and the radiation and reception of pulses by antennas.

Dr. Smith is a member of Tau Beta Pi, Eta Kappa Nu, and Sigma Xi, and URSI Commissions A and B.

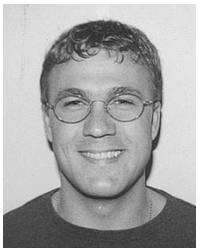

L. E. Rickard Petersson (S'96) was born in Örebro, Sweden, on May 15, 1972. He received the B.S.E.E degree from Tennessee Technological University, Cookeville, TN, in 1997, and the M.S. degree in electrical and computer engineering from the Georgia Institute of Technology, Atlanta, GA, in 1999. He is currently working toward the Ph.D. degree at the Georgia Institute of Technology.

His special research interests include electromagnetic analysis using spectral techniques and numerical modeling.